Available online at www.sciencedirect.com
ScienceDirect
International Journal of Multiphase Flow 34 (2008) 42–60
International Journal of Multiphase Flow
www.elsevier.com/locate/ijmulflow

Instability of a viscoelastic liquid jet with axisymmetric and asymmetric disturbances

Zhihao Liu [a], Zhengbai Liu [b,*]

[a] Microsoft Corporation, One Microsoft Way, Redmond, WA 98052, USA
[b] International Truck and Engine Corporation, 10400 W. North Avenue, Melrose Park, IL 60160, USA

Received 5 September 2006; received in revised form 6 August 2007

Abstract

The temporal instability behavior of a viscoelastic liquid jet in the wind-induced regime with axisymmetric and asymmetric disturbances moving in an inviscid gaseous environment is investigated theoretically. The corresponding dispersion relation between the wave growth rate and the wavenumber is derived. The linear instability analysis shows that viscoelastic liquid jets are more unstable than their Newtonian counterparts, and less unstable than their inviscid counterparts, for both axisymmetric and asymmetric disturbances, respectively. The instability behavior of viscoelastic jets is influenced by the interaction of liquid viscosity and elasticity, in which the viscosity tends to dampen the instability, whereas the elasticity results in an enhancement of instability. Relatively, the effect of the ratio of deformation retardation to stress relaxation time on the instability of viscoelastic jets is weak. It is found that the liquid Weber number is a key measure that controls the viscoelastic jet instability behavior. At small Weber number, the axisymmetric disturbance dominates the instability of viscoelastic jets, i.e., the growth rate of an axisymmetric disturbance exceeds that of asymmetric disturbances. When the Weber number increases, both the growth rate and the instability range of disturbances increase drastically. The asymptotic analysis shows that at large Weber number, more asymmetric disturbance modes become unstable, and the growth rate of each asymmetric disturbance mode approaches that of the axisymmetric disturbance. Therefore, the asymmetric disturbances are more dangerous than that of axisymmetric disturbances for a viscoelastic jet at large Weber numbers. Similar to the liquid Weber number, the ratio of gas to liquid density is another key measure that affects the viscoelastic jet instability behavior substantially.

Keywords: Instability; Viscoelastic liquid jets; Asymmetric disturbances

1. Introduction

Breakup of a liquid jet into droplets has been involved in many practical applications such as in diesel engines, gas turbine engines, liquid rocket engines, oil burners, spray coating process, plastics manufacture,

* Corresponding author. Tel.: +1 708 865 3759; fax: +1 708 865 4043.
E-mail address: mike.liu@nav-international.com (Z. Liu).

0301-9322/$ - see front matter © 2007 Elsevier Ltd. All rights reserved.
doi:10.1016/j.ijmultiphaseflow.2007.08.001

metal powder production, lubrication, and so on. Therefore, it is of interest and importance to understand the mechanisms of instability and breakup of liquid jets, since the efficiency and quality of production is strongly dependent on these mechanisms.

The capillary instability of liquid jets has been the subject of numerous studies since 19th century. Rayleigh (1878, 1879) considered the capillary stability of a cylinder of an inviscid fluid, and he also discussed the case of a viscous liquid jet without inertia (Rayleigh, 1892). Weber (1931) obtained the complete linear solution for a viscous liquid jet under surface tension forces in which he also included the action of an inviscid atmosphere. Since then, more experimental and theoretical investigations on mechanisms of liquid jet instability have been performed by Middleman (1965), Yuen (1968), Kroesser and Middleman (1969), Goedde and Yuen (1970), McCarthy and Molloy (1974), Bogy (1979), and Chigier and Reitz (1996), and different theories have been proposed to explain the instability behavior. The theory of aerodynamic interaction between the liquid jet and the ambient gas assumes that the instability is due to aerodynamic interaction between the liquid and the ambient gas, which induces unstable wave growth on the liquid surface. The growth of these unstable waves eventually breaks up the liquid jet into ligaments, and then small drops (Li, 1995). Reitz and Bracco (1982) found that the theory of aerodynamic interaction leading to surface wave growth is compatible with their measurements for a given nozzle. Consequently, the effects of aerodynamic interaction on the instability behavior have been explored in great detail, and the interfacial pressure fluctuations have been identified as the vehicle for the development of the unstable wave growth on the jet surface (Lin and Kang, 1987; Zhou and Lin, 1992; Lian and Reitz, 1993).

So far, considerable literature is available on the liquid jet instability (Giffen and Muraszew, 1953; Batchelor and Gill, 1962; Grant and Middleman, 1966; Meister and Scheele, 1969; Phinney, 1973), which is very helpful to understand the mechanisms of the instability and breakup of liquid jets for Newtonian fluids. However, things are more difficult for viscoelastic jets due to the differences in liquid behavior (Darby, 1976; Schowalter, 1978; Yarin, 1993). On the other hand, in the studies of jet instability, it is regarded that axisymmetric disturbances are always more detrimental than asymmetric ones (Sterling and Sleicher, 1975; Lin and Lian, 1990; Lin and Ibrahim, 1990; Brenn et al., 2000; Liu and Liu, 2006). As a result, most of the investigations are focused on the axisymmetric instability of liquid jets. It is therefore that there is a need to investigate the instability characteristics of viscoelastic liquid jets with asymmetric disturbances.

The objective of the present paper is to extend the work on Newtonian jets done by Li (1995), i.e., to investigate the mechanisms of temporal instability of viscoelastic liquid jets with both axisymmetric and asymmetric disturbances, and to explore the differences between the instabilities of axisymmetric and asymmetric disturbances, concentrating on the wind-induced regime. It is hoped that the present work can provide a good foundation for further investigations of the instability and breakup of viscoelastic liquid jets. Hence, in the following sections the dispersion relation between the growth rate and the wavenumber for a viscoelastic liquid jet with three-dimensional disturbances are derived in detail. Then, the effects of various parameters on the instability behavior are studied. Finally, a number of quantitative conclusions on the instability behavior of viscoelastic jets with both axisymmetric and asymmetric disturbances are summarized.

2. Theory

Consider a cylindrical jet of viscoelastic liquid of density ρ, surface tension σ, and radius a moving at velocity $\overline{U}$ through an inviscid gas of density ρ_g. The governing equations are written in a cylindrical coordinate system for convenience. The coordinates are chosen such that the z-axis is parallel to the moving direction of the liquid jet flow, the r-axis is normal to the liquid jet with its origin located on the jet axis, and the θ-axis is in the azimuthal direction.

2.1. Liquid phase velocity and pressure distribution

The governing equations of the liquid motion in a jet are the conservation laws of mass and momentum, as given below:

$$\frac{\partial \rho}{\partial t} + \nabla \cdot \rho \mathbf{v} = 0, \tag{1}$$

$$\rho\left(\frac{\partial}{\partial t} + \mathbf{v} \cdot \nabla\right)\mathbf{v} = -\nabla \cdot \boldsymbol{\pi} + \rho \mathbf{g}, \tag{2}$$

where t is the time, $\mathbf{v}$ is the liquid velocity vector, $\mathbf{g}$ is the gravitational acceleration vector, and $\boldsymbol{\pi}$ is the total stress tensor of the liquid, which is given by

$$\boldsymbol{\pi} = p\boldsymbol{\delta} + \boldsymbol{\tau}, \tag{3}$$

where p is the pressure of the liquid due to the disturbance, $\boldsymbol{\tau}$ is the extra stress tensor of the liquid, and $\boldsymbol{\delta}$ is the unit tensor.

A corotational Oldroyd eight-constant model is used for describing the viscoelastic liquid state (Bird et al., 1977; Park and Lee, 1995; Goren and Gottlieb, 1982; Liu et al., 1998). The following linearized equations are obtained after neglecting the nonlinear terms and gravitational effects:

$$\nabla \cdot \mathbf{v} = 0, \tag{4}$$

$$\rho\left(\frac{\partial}{\partial t} + \overline{U}\frac{\partial}{\partial z}\right)\mathbf{v} = -\nabla \cdot (p\boldsymbol{\delta} + \boldsymbol{\tau}), \tag{5}$$

$$\boldsymbol{\tau} + \lambda_1\left(\frac{\partial}{\partial t} + \overline{U}\frac{\partial}{\partial z}\right)\boldsymbol{\tau} = -\eta_0\left[\dot{\boldsymbol{\gamma}} + \lambda_2\left(\frac{\partial}{\partial t} + \overline{U}\frac{\partial}{\partial z}\right)\dot{\boldsymbol{\gamma}}\right], \tag{6}$$

where $\dot{\gamma}$ is the strain tensor, η_0 is the zero shear viscosity, λ_1 is the stress relaxation time, and λ_2 is the deformation retardation time.

As the jet issues from the nozzle, the jet surface is always subjected to disturbances. The equation for the jet surface disturbed by a small disturbance is expressed as follows:

$$r = a + \xi, \tag{7}$$

where $r = a$ is the equilibrium position of the jet surface, i.e., the position without disturbances, and ξ is the displacement of a point on the surface.

Since we are interested in the wave motion in the liquid, we seek the solutions for the velocity vector $\mathbf{v}$ as periodic functions in z and θ, and complex exponential functions in t:

$$\mathbf{v} = \mathbf{V}(r)\mathrm{e}^{\mathrm{i}(kz+n\theta)+\alpha t}, \tag{8}$$

and the velocity vector $\mathbf{v}$ has three components, that is:

$$v_r = V_r(r)\mathrm{e}^{\mathrm{i}(kz+n\theta)+\alpha t}, \tag{9}$$

$$v_\theta = V_\theta(r)\mathrm{e}^{\mathrm{i}(kz+n\theta)+\alpha t}, \tag{10}$$

$$v_z = V_z(r)\mathrm{e}^{\mathrm{i}(kz+n\theta)+\alpha t}, \tag{11}$$

where α is a complex frequency ($\alpha = \alpha_r + \mathrm{i}\alpha_i$, where α_r represents the wave growth rate of the disturbance, α_i is 2π times the disturbance frequency, and $-\alpha_i/k$ is the wave propagation velocity of the disturbance in the direction of the liquid flow), k is real, representing the wavenumber of the disturbance in z direction, and n is an integer, representing the disturbance mode.

It is n in the above expression that introduces the effects of the asymmetric disturbances. It should be noted that when $n = 0$, the interfacial waves on the jet surface correspond to symmetrical jet surface deformations with successive contractions and expansions in radial direction, and are called varicose waves. A schematic diagram of a liquid jet for the varicose disturbances is shown in Fig. 1a. When $n = 1$, the interfacial waves on the jet surface correspond to the jet surface deformation in which the cross section remains circular but is displaced relative to the jet axis, and are referred to sinuous waves. A schematic diagram of a liquid jet for the sinuous disturbances is shown in Fig. 1b. When $n = 2$, the jet develops elliptical cross sections. An ellipse with a horizontal major axis is transformed successively into an ellipse with a vertical major axis, and vice versa. When $n \geqslant 3$, sinusoidal surface deformations occur in both the axial and azimuthal directions,

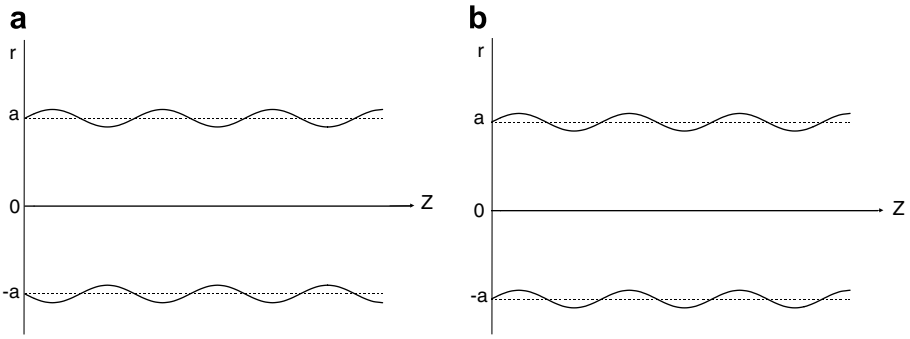

Fig. 1. Schematic diagram of a liquid jet for the laboratory-fixed coordinate system (r, θ, z) for (a) the varicose disturbances ($n = 0$) and (b) the sinuous disturbances ($n = 1$).

and become more and more complicated as unstable waves with larger values of n set in and start to grow on the jet surface.

Thus, the stress tensor $\boldsymbol{\tau}$, the strain tensor $\dot{\boldsymbol{\gamma}}$, the pressure p, and the interface displacement ξ are periodic functions in z and θ, and exponential functions in t, i.e.,

$$\boldsymbol{\tau} = \mathbf{T}(r)\mathrm{e}^{\mathrm{i}(kz+n\theta)+\alpha t}, \tag{12}$$

$$\dot{\boldsymbol{\gamma}} = \dot{\boldsymbol{\Gamma}}(r)\mathrm{e}^{\mathrm{i}(kz+n\theta)+\alpha t}, \tag{13}$$

$$p = P(r)\mathrm{e}^{\mathrm{i}(kz+n\theta)+\alpha t}, \tag{14}$$

$$\xi = \xi_0\mathrm{e}^{\mathrm{i}(kz+n\theta)+\alpha t}, \tag{15}$$

where ξ_0 is the initial amplitude of the disturbance, which is thought to be much smaller than the radius a of the jet in the linear stability theory.

Differentiating Eqs. (12) and (13), and substituting the results into Eq. (6) results in

$$\boldsymbol{\tau} = -\eta(\alpha)\dot{\boldsymbol{\gamma}}, \tag{16}$$

where

$$\eta(\alpha) = \eta_0\frac{1+\lambda_2(\alpha+\mathrm{i}k\overline{U})}{1+\lambda_1(\alpha+\mathrm{i}k\overline{U})}. \tag{17}$$

Substituting Eq. (16) into Eq. (5), and expressing the governing equations and the velocity vector in suitable component forms, the following scalar continuity and momentum equations are obtained in cylindrical coordinates,

$$\frac{1}{r}\frac{\partial}{\partial r}(rv_r) + \frac{1}{r}\frac{\partial}{\partial\theta}(v_\theta) + \frac{\partial v_z}{\partial z} = 0, \tag{18}$$

$$\rho\left(\frac{\partial v_r}{\partial t} + \overline{U}\frac{\partial v_r}{\partial z}\right) = -\frac{\partial p}{\partial r} + \eta(\alpha)\left\{\frac{\partial}{\partial r}\left[\frac{1}{r}\frac{\partial}{\partial r}(rv_r)\right] + \frac{1}{r^2}\frac{\partial^2 v_r}{\partial\theta^2} - \frac{2}{r^2}\frac{\partial v_\theta}{\partial\theta} + \frac{\partial^2 v_r}{\partial z^2}\right\}, \tag{19}$$

$$\rho\left(\frac{\partial v_\theta}{\partial t} + \overline{U}\frac{\partial v_\theta}{\partial z}\right) = -\frac{1}{r}\frac{\partial p}{\partial\theta} + \eta(\alpha)\left\{\frac{\partial}{\partial r}\left[\frac{1}{r}\frac{\partial}{\partial r}(rv_\theta)\right] + \frac{1}{r^2}\frac{\partial^2 v_\theta}{\partial\theta^2} + \frac{2}{r^2}\frac{\partial v_r}{\partial\theta} + \frac{\partial^2 v_\theta}{\partial z^2}\right\}, \tag{20}$$

$$\rho\left(\frac{\partial v_z}{\partial t} + \overline{U}\frac{\partial v_z}{\partial z}\right) = -\frac{\partial p}{\partial z} + \eta(\alpha)\left\{\frac{1}{r}\frac{\partial}{\partial r}\left(r\frac{\partial v_z}{\partial r}\right) + \frac{1}{r^2}\frac{\partial^2 v_z}{\partial\theta^2} + \frac{\partial^2 v_z}{\partial z^2}\right\}. \tag{21}$$

The flow field solutions of the above governing equations have to satisfy the kinematic and dynamic boundary conditions at the gas–liquid interface, which can be taken to be $r = a$ (the first order approximation for a small displacement of the interface due to the disturbance). Thus, in mathematical form, the kinematic boundary condition requires that

$$v_r = \frac{\partial \xi}{\partial t} + \overline{U}\frac{\partial \xi}{\partial z}, \quad r = a, \tag{22}$$

and the dynamic boundary conditions require that

$$\pi_{rz} = \tau_{rz} = -\eta(\alpha)\left(\frac{\partial v_z}{\partial r} + \frac{\partial v_r}{\partial z}\right) = 0, \quad r = a, \tag{23}$$

$$\pi_{r\theta} = \tau_{r\theta} = -\eta(\alpha)\left[r\frac{\partial}{\partial r}\left(\frac{v_\theta}{r}\right) + \frac{1}{r}\frac{\partial v_r}{\partial \theta}\right] = 0, \quad r = a, \tag{24}$$

$$\pi_{rr} - \pi_{g,rr} + p_\sigma = 0, \quad r = a, \tag{25}$$

where subscript 'g' denotes the gas phase, π_{rr} is the liquid normal stress, $\pi_{g,rr}$ is the gas normal stress, and p_σ is the pressure induced by the surface tension. Moreover, the velocity components along the jet axis, i.e., at $r = 0$, must be finite.

Solving differential Eqs. (18)–(21) and applying the boundary conditions (22)–(24), the final forms of the pressure and velocity profiles in the liquid read:

$$p = -\frac{C_1}{C_2}(\alpha + \mathrm{i}k\overline{U})^2\frac{\rho}{k}\frac{I_n(kr)}{I'_n(ka)}\frac{l^2+k^2}{l^2-k^2}\xi_0 e^{\mathrm{i}(kz+n\theta)+\alpha t}, \tag{26}$$

$$v_r = \frac{(\alpha + \mathrm{i}k\overline{U})}{C_2}\left[C_1\frac{I'_n(kr)}{I'_n(ka)} + \frac{2aC_3}{r}\frac{I'_n(lr)}{I_n(la)} - \frac{2k^2C_4}{l^2+k^2}\frac{I'_n(lr)}{I'_n(la)}\right]\frac{l^2+k^2}{l^2-k^2}\xi_0 e^{\mathrm{i}(kz+n\theta)+\alpha t}, \tag{27}$$

$$v_\theta = \frac{\mathrm{i}(\alpha + \mathrm{i}k\overline{U})}{C_2}\left[\frac{nC_1}{kr}\frac{I_n(kr)}{I'_n(ka)} + \frac{2laC_3}{n}\frac{I'_n(lr)}{I_n(la)} - \frac{2nk^2C_4}{l^2+k^2}\frac{1}{lr}\frac{I_n(lr)}{I'_n(la)}\right]\frac{l^2+k^2}{l^2-k^2}\xi_0 e^{\mathrm{i}(kz+n\theta)+\alpha t}, \tag{28}$$

$$v_z = \frac{\mathrm{i}(\alpha + \mathrm{i}k\overline{U})}{C_2}\left[\frac{C_1}{I'_n(ka)}I_n(kr) - \frac{2klC_4}{(l^2+k^2)I'_n(la)}I_n(lr)\right]\frac{l^2+k^2}{l^2-k^2}\xi_0 e^{\mathrm{i}(kz+n\theta)+\alpha t}, \tag{29}$$

where $I_n(kr)$ is the nth order modified Bessel function of the first kind, and

$$l^2 = k^2 + \frac{\rho(\alpha + \mathrm{i}k\overline{U})}{\eta(\alpha)}, \tag{30}$$

$$C_1 = la\frac{I'_n(la)}{I_n(la)} - l^2a^2\frac{I''_n(la)}{I_n(la)} - \frac{n^2}{l^2+k^2}\left[(l^2-k^2) + \frac{2k^2}{la}\frac{I_n(la)}{I'_n(la)}\right], \tag{31}$$

$$C_2 = la\frac{I'_n(la)}{I_n(la)} - l^2a^2\frac{I''_n(la)}{I_n(la)} + \frac{2n^2}{l^2-k^2}\left[\frac{l^2-k^2}{2} + \frac{k^2}{la}\frac{I_n(la)}{I'_n(la)} - \frac{l^2}{ka}\frac{I_n(ka)}{I'_n(ka)}\right], \tag{32}$$

$$C_3 = \frac{n^2}{l^2+k^2}\left[(l^2-k^2) - \frac{l^2+k^2}{ka}\frac{I_n(ka)}{I'_n(ka)} + \frac{2k^2}{la}\frac{I_n(la)}{I'_n(la)}\right], \tag{33}$$

$$C_4 = la\frac{I'_n(la)}{I_n(la)} - l^2a^2\frac{I''_n(la)}{I_n(la)} - \frac{n^2}{ka}\frac{I_n(ka)}{I'_n(ka)}. \tag{34}$$

2.2. Gas phase velocity and pressure distribution

In the present analysis the gas around the moving liquid jet is assumed to be inviscid, and it moves at a velocity $\overline{U}_g$ in the same direction as the flow of the liquid jet. Similar to the liquid phase, the governing equations for the gas phase are expressed as follows:

$$\frac{1}{r}\frac{\partial}{\partial r}(rv_{r,g}) + \frac{1}{r}\frac{\partial}{\partial \theta}(v_{\theta,g}) + \frac{\partial v_{z,g}}{\partial z} = 0, \tag{35}$$

$$\rho_g\left(\frac{\partial v_{r,g}}{\partial t} + \overline{U}_g\frac{\partial v_{r,g}}{\partial z}\right) = -\frac{\partial p_g}{\partial r}, \tag{36}$$

$$\rho_g\left(\frac{\partial v_{\theta,g}}{\partial t} + \overline{U}_g\frac{\partial v_{\theta,g}}{\partial z}\right) = -\frac{1}{r}\frac{\partial p_g}{\partial \theta}, \tag{37}$$

$$\rho_{\mathrm{g}}\left(\frac{\partial v_{z,\mathrm{g}}}{\partial t}+\overline{U}_{\mathrm{g}}\frac{\partial v_{z,\mathrm{g}}}{\partial z}\right)=-\frac{\partial p_{\mathrm{g}}}{\partial z}, \tag{38}$$

where Eq. (35) is the gas phase continuity equation, and Eqs. (36)–(38) are the gas phase momentum equations. The boundary conditions for the gas phase are regarded as

$$v_{r,\mathrm{g}}=\frac{\partial \xi}{\partial t}+\overline{U}_{\mathrm{g}}\frac{\partial \xi}{\partial z}, \quad r=a, \tag{39}$$

$$v_{r,\mathrm{g}}=0, \quad r\to\infty. \tag{40}$$

The same calculation as for the liquid phase leads to the final form of the profiles of the pressure and three velocity components in the gas phase.

$$p_{\mathrm{g}}=-\frac{\rho_{\mathrm{g}}}{k}\frac{(\alpha+\mathrm{i}k\overline{U}_{\mathrm{g}})^2}{K_n'(ka)}K_n(kr)\xi_0\mathrm{e}^{\mathrm{i}(kz+n\theta)+\alpha t}, \quad r\geqslant a, \tag{41}$$

$$v_{r,\mathrm{g}}=\frac{(\alpha+\mathrm{i}k\overline{U}_{\mathrm{g}})}{K_n'(ka)}K_n'(kr)\xi_0\mathrm{e}^{\mathrm{i}(kz+n\theta)+\alpha t}, \quad r\geqslant a, \tag{42}$$

$$v_{\theta,\mathrm{g}}=\frac{\mathrm{i}n}{k}\frac{(\alpha+\mathrm{i}k\overline{U}_{\mathrm{g}})}{K_n'(ka)}\frac{1}{r}K_n(kr)\xi_0\mathrm{e}^{\mathrm{i}(kz+n\theta)+\alpha t}, \quad r\geqslant a, \tag{43}$$

$$v_{z,\mathrm{g}}=\mathrm{i}\frac{(\alpha+\mathrm{i}k\overline{U}_{\mathrm{g}})}{K_n'(ka)}K_n(kr)\xi_0\mathrm{e}^{\mathrm{i}(kz+n\theta)+\alpha t}, \quad r\geqslant a, \tag{44}$$

where $K_n(kr)$ is the nth order modified Bessel function of the second kind.

2.3. Dispersion relation

The normal stress in the liquid jet can be obtained from the corresponding equations of the velocity and pressure profiles.

$$\begin{aligned}\pi_{rr}&=p+\tau_{rr}=p-2\eta(\alpha)\frac{\partial v_r}{\partial r}\\&=\left\{-\frac{\rho C_1}{k}\frac{I_n(kr)}{I_n'(ka)}(\alpha+\mathrm{i}k\overline{U})^2-2\eta(\alpha)\left[kC_1\frac{I_n''(kr)}{I_n'(ka)}+\frac{2aC_3}{r^2}\left[\frac{lrI_n''(lr)}{I_n(la)}-\frac{I_n'(lr)}{I_n(la)}\right]\right.\right.\\&\quad\left.\left.-\frac{2k^2lC_4}{l^2+k^2}\frac{I_n''(lr)}{I_n'(la)}\right](\alpha+\mathrm{i}k\overline{U})\right\}\frac{l^2+k^2}{l^2-k^2}\frac{\xi_0}{C_2}\mathrm{e}^{\mathrm{i}(kz+n\theta)+\alpha t}, \quad r\leqslant a.\end{aligned} \tag{45}$$

The normal stress in the gas is obtained from $\pi_{\mathrm{g},rr}=p_{\mathrm{g}}$

$$\pi_{\mathrm{g},rr}=-\frac{\rho_{\mathrm{g}}(\alpha+\mathrm{i}k\overline{U}_{\mathrm{g}})^2}{k}\frac{K_n(kr)}{K_n'(ka)}\xi_0\mathrm{e}^{\mathrm{i}(kz+n\theta)+\alpha t}, \quad r\geqslant a. \tag{46}$$

The pressure induced by the surface tension to the first order in ξ is expressed as

$$p_\sigma=\frac{\sigma}{a^2}\left(\xi+a^2\frac{\partial^2\xi}{\partial z^2}+\frac{\partial^2\xi}{\partial\theta^2}\right)=\frac{\sigma}{a^2}(1-k^2a^2-n^2)\xi_0\mathrm{e}^{\mathrm{i}(kz+n\theta)+\alpha t}. \tag{47}$$

Substituting the expressions found for π_{rr}, $\pi_{\mathrm{g},rr}$, and p_σ into the normal stress boundary condition (25) for $r=a$ yields the following dispersion relation:

$$(\alpha+\mathrm{i}k\overline{U})^2+\frac{2k^2\eta_0}{\rho}\frac{1+\lambda_2(\alpha+\mathrm{i}k\overline{U})}{1+\lambda_1(\alpha+\mathrm{i}k\overline{U})}\left\{\frac{I_n''(ka)}{I_n(ka)}+\frac{C_3}{C_1}\frac{2}{ka}\left[la\frac{I_n''(la)}{I_n(la)}-\frac{I_n'(la)}{I_n(la)}\right]\frac{I_n'(ka)}{I_n(ka)}\right.$$
$$\left.-\frac{C_4}{C_1}\frac{2kl}{l^2+k^2}\frac{I_n''(la)}{I_n'(la)}\frac{I_n'(ka)}{I_n(ka)}\right\}(\alpha+\mathrm{i}k\overline{U})-\frac{C_2}{C_1}\frac{\rho_g}{\rho}\frac{l^2-k^2}{l^2+k^2}\frac{K_n(ka)}{K_n'(ka)}\frac{I_n'(ka)}{I_n(ka)}(\alpha+\mathrm{i}k\overline{U}_g)^2$$
$$=\frac{C_2}{C_1}\frac{\sigma k}{\rho a^2}\frac{l^2-k^2}{l^2+k^2}(1-k^2a^2-n^2)\frac{I_n'(ka)}{I_n(ka)}. \tag{48}$$

Eq. (48) relates the wave growth rate α to the wavenumber k, but its solution is complicated by the fact that the parameter l is still a function of α.

When $\lambda_1=\lambda_2=0$, the jet of a viscoelastic fluid is transformed into that of a Newtonian fluid (at this condition $\eta_0=\mu$, where $\mu=\nu\rho$ is the dynamic viscosity of the Newtonian fluid, and ν is the kinematic viscosity of the Newtonian fluid), and the dispersion relation (48) reduces to the results for a Newtonian fluid:

$$(\alpha+\mathrm{i}k\overline{U})^2+2\nu k^2\left[\frac{I_n''(ka)}{I_n(ka)}+\frac{C_3}{C_1}\frac{2}{ka}\left[la\frac{I_n''(la)}{I_n(la)}-\frac{I_n'(la)}{I_n(la)}\right]\frac{I_n'(ka)}{I_n(ka)}-\frac{C_4}{C_1}\frac{2kl}{l^2+k^2}\frac{I_n''(la)}{I_n'(la)}\frac{I_n'(ka)}{I_n(ka)}\right](\alpha+\mathrm{i}k\overline{U})$$
$$-\frac{C_2}{C_1}\frac{\rho_g}{\rho}\frac{l^2-k^2}{l^2+k^2}\frac{K_n(ka)}{K_n'(ka)}\frac{I_n'(ka)}{I_n(ka)}(\alpha+\mathrm{i}k\overline{U}_g)^2=\frac{C_2}{C_1}\frac{\sigma k}{\rho a^2}\frac{l^2-k^2}{l^2+k^2}(1-k^2a^2-n^2)\frac{I_n'(ka)}{I_n(ka)}. \tag{49}$$

When the liquid viscosity vanishes, the jet of a Newtonian fluid is transformed into that of an inviscid fluid, and the dispersion relation (49) reduces to the results for an inviscid fluid.

$$(\alpha+\mathrm{i}k\overline{U})^2-\frac{\rho_g}{\rho}\frac{K_n(ka)}{K_n'(ka)}\frac{I_n'(ka)}{I_n(ka)}(\alpha+\mathrm{i}k\overline{U}_g)^2=\frac{\sigma k}{\rho a^2}(1-k^2a^2-n^2)\frac{I_n'(ka)}{I_n(ka)}. \tag{50}$$

When $n=0$, the above three-dimensional dispersion relations can reduce to the corresponding two-dimensional (axisymmetric) forms, respectively, for viscoelastic fluid (Brenn et al., 2000), Newtonian one (Weber, 1931), and inviscid one (Rayleigh, 1879).

From the above derivations, it is seen that the three-dimensional viscoelastic liquid jet dispersion relation recovers the dispersion relations for the jets of the three-dimensional Newtonian and inviscid fluids as well as two-dimensional analogs, thus confirming the validity of the three-dimensional viscoelastic linear solution. The following work analyzes the three-dimensional instability of the viscoelastic liquid jets by using the dispersion relation (48).

3. Results

For convenience, the above dispersion relation of a viscoelastic liquid jet, Eq. (48), can be expressed in non-dimensional form as

$$\Omega_1^2+2K^2Z\frac{Z+\tilde{\lambda}El\Omega_1}{Z+El\Omega_1}\left\{\frac{I_n''(K)}{I_n(K)}+\frac{C_3}{C_1}\frac{2}{K}\left[L\frac{I_n''(L)}{I_n(L)}-\frac{I_n'(L)}{I_n(L)}\right]\frac{I_n'(K)}{I_n(K)}-\frac{C_4}{C_1}\frac{2KL}{L^2+K^2}\frac{I_n''(L)}{I_n'(L)}\frac{I_n'(K)}{I_n(K)}\right\}\Omega_1$$
$$-C\frac{C_2}{C_1}\tilde{\rho}\frac{L^2-K^2}{L^2+K^2}\frac{K_n(K)}{K_n'(K)}\frac{I_n'(K)}{I_n(K)}\Omega_2^2=\frac{C_2}{C_1}K\frac{L^2-K^2}{L^2+K^2}(1-K^2-n^2)\frac{I_n'(K)}{I_n(K)}, \tag{51}$$

where

$$L^2=K^2+\frac{\Omega_1}{Z}\frac{Z+El\Omega_1}{Z+\tilde{\lambda}El\Omega_1}, \tag{52}$$

$$C_1=L\frac{I_n'(L)}{I_n(L)}-L^2\frac{I_n''(L)}{I_n(L)}-\frac{n^2}{L^2+K^2}\left[(L^2-K^2)+\frac{2K^2}{L}\frac{I_n(L)}{I_n'(L)}\right], \tag{53}$$

$$C_2 = L\frac{I_n'(L)}{I_n(L)} - L^2\frac{I_n''(L)}{I_n(L)} + \frac{2n^2}{L^2-K^2}\left[\frac{L^2-K^2}{2} + \frac{K^2}{L}\frac{I_n(L)}{I_n'(L)} - \frac{L^2}{K}\frac{I_n(K)}{I_n'(K)}\right], \tag{54}$$

$$C_3 = \frac{n^2}{L^2+K^2}\left[(L^2-K^2) - \frac{L^2+K^2}{K}\frac{I_n(K)}{I_n'(K)} + \frac{2K^2}{L}\frac{I_n(L)}{I_n'(L)}\right], \tag{55}$$

$$C_4 = L\frac{I_n'(L)}{I_n(L)} - L^2\frac{I_n''(L)}{I_n(L)} - \frac{n^2}{K}\frac{I_n(K)}{I_n'(K)}, \tag{56}$$

and $\Omega_1 = \Omega + \mathrm{i}K(We)^{1/2}$, $\Omega_2 = \Omega + \mathrm{i}K\widetilde{U}(We)^{1/2}$, $\Omega = \Omega_r + \mathrm{i}(We)^{1/2}\Omega_i$, $\Omega_r = \alpha_r/(\sigma/\rho a^3)^{1/2}$ is the non-dimensional growth rate, $\Omega_i = \alpha_i/(\overline{U}/a)$ is the non-dimensional disturbance frequency, $K = ka$ is the non-dimensional (real) wavenumber, $L = la$, $\tilde{\rho} = \rho_g/\rho$ is the ratio of gas density to liquid density, $\widetilde{U} = \overline{U}_g/\overline{U}$ is the ratio of gas velocity to liquid velocity, $\tilde{\lambda} = \lambda_2/\lambda_1$ is the ratio of deformation retardation time to stress relaxation time (the time constant ratio for short). The liquid Weber number is defined as $We = \rho\overline{U}^2 a/\sigma$, which represents the ratio of inertial force to surface tension force. The Reynolds number is defined as $Re = \rho\overline{U}a/\eta_0$, which expresses the ratio of inertial force to viscous force, the Ohnesorge number is defined as $Z = \eta_0/(\rho\sigma a)^{1/2}$, which denotes the ratio of viscous force to surface tension force. The elasticity number is defined as $El = \lambda_1\eta_0/\rho a^2$, which represents a relationship between viscous effect and elastic effect in the liquid. The constant C in front of the aerodynamic term in the dispersion relation is introduced to consider the effect of gas viscous due to Sterling and Sleicher (1975), and Gordillo and Perez-Saborid (2005). According to Sterling and Sleicher (1975), the value of the constant $C = 0.175$.

The instability of liquid jets corresponds to positive values of the disturbance growth rate (i.e., $\alpha_r > 0$ or $\Omega_r > 0$), and the growth rate of disturbances on liquid jets can be obtained through solving the above corresponding dispersion relations by using Muller's secant method (1956).

Gordon et al. (1973) showed the dispersion relation for a jet of an aqueous 0.05% Separan AP30 solution. Separan is a polyacrylamide frequently used in experiments on viscoelastic jets. Its ratio of deformation retardation time to stress relaxation time is $\tilde{\lambda} = 0.1$. To make our concentration on the wind-induced regime and for the general case, the non-dimensional wave growth rate Ω_r of disturbances on different liquid jets versus the non-dimensional wavenumber K at $Z = 0.1$, $Re = 2236$, $We = 50\,000$, $El = 0.1$, $\tilde{\lambda} = 0.1, \tilde{\rho} = 0.001$, and $\overline{U}_g = 0$ is calculated and shown in Fig. 2a for $n = 0$ and $n = 2$, and in Fig. 2b for $n = 1$ and $n = 3$. The asymmetric (three-dimensional) results are obtained from the dispersion relations with $n = 1$, 2, and 3, and the axisymmetric (two-dimensional) results are attained from the dispersion relations with $n = 0$. It should be noted that any value of n other than zero would correspond to an asymmetric disturbance mode and thus cause the disturbance to be three-dimensional.

The cutoff wavenumber is the value where the growth rate curve crosses the wavenumber axis in the plot of wave growth rate versus wavenumber, and it is obtained from the corresponding dispersion relations by setting $\alpha_r = 0$ or $\Omega_r = 0$. From inspection of Fig. 2, it is found that the most obvious difference between axisymmetric and asymmetric disturbances is that, in addition to an upper cutoff wavenumber, asymmetric disturbances exhibit a lower cutoff wavenumber as well. Below the lower cutoff wavenumber or above the upper cutoff wavenumber, the growth rates are negative. Therefore, the liquid jet is stable. Only those disturbances with wavenumbers between the lower and upper cutoff wavenumbers are unstable. In this sense, the lower cutoff wavenumber for axisymmetric disturbances may also be regarded to exist, as zero, corresponding to disturbances of infinitely long wavelength. It is further discovered that except for $n = 1$, a non-zero lower cutoff wavenumber exists for all other asymmetric disturbances ($n > 1$), and increases with n, whereas the upper cutoff wavenumber decreases with n. This is not only the characteristic of asymmetric disturbances in the instability of viscoelastic liquid jets, but also the characteristic of asymmetric disturbances in the instability of Newtonian and inviscid liquid jets. Similar results were reported by Li (1995) in his studies on the instability of Newtonian liquid jets. In addition, it is also evident from Fig. 2 that for the given flow condition the maximum growth rate and the corresponding dominant wavenumber decrease as the value of n increases. Therefore, when n is greater than some value for a given condition, the growth rates become negative and the corresponding asymmetric disturbances are stable. For the condition in Fig. 2, the asymmetric disturbances are stable at $n > 3$ for the jets of three types of fluids. It is also discovered that for the same liquid Weber num-

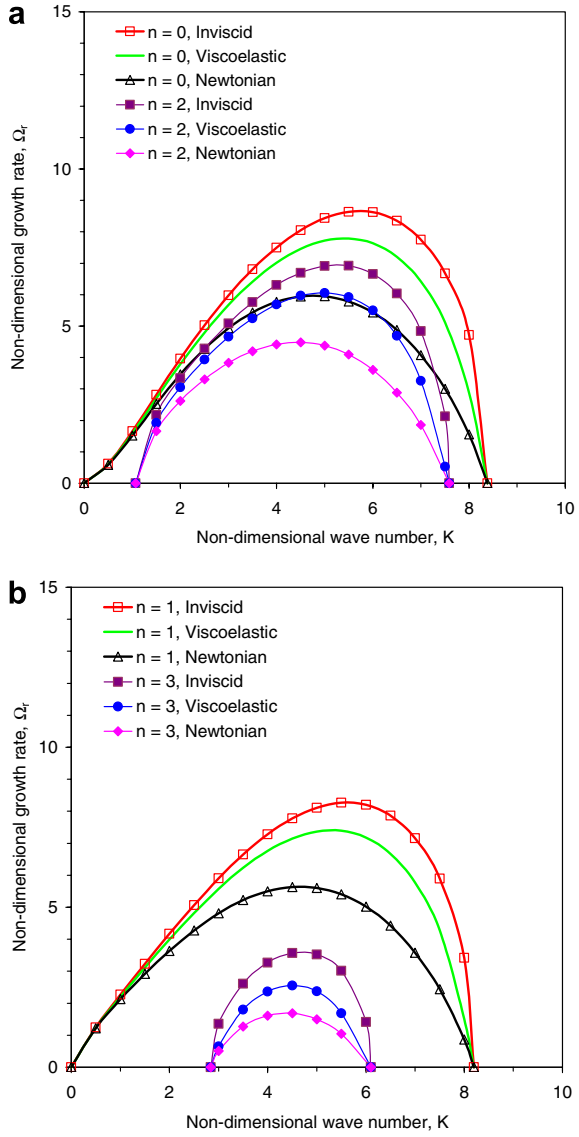

Fig. 2. Wave growth rate Ω_r of axisymmetric and asymmetric disturbances on different liquid jets versus wavenumber K at $Z = 0.1$, $Re = 2236$, $We = 50000$, $El = 0.1$, $\tilde{\lambda} = 0.1$, $\tilde{\rho} = 0.001$, and $\overline{U}_g = 0$ for (a) $n = 0$ and $n = 2$, and (b) $n = 1$ and $n = 3$.

ber the unstable wavenumber range is almost identical for each corresponding disturbance mode on jets of viscoelastic, Newtonian, and inviscid fluids.

From inspection of the curve shapes of wave growth rate of different disturbances in Fig. 2, it is seen that for relatively small wavenumbers, the axisymmetric growth rate curve is convex, and the asymmetric growth rate curves are always concave. Three types of fluids demonstrate the same feature. In addition, Fig. 2 also shows the effects of the value of n on the growth rate of disturbances on a different liquid jets. It is observed from this figure that the maximum growth rate of the axisymmetric disturbance exceeds that of the asymmetric disturbances. It is further noticed that the asymmetric disturbance corresponding to $n = 1$ possesses higher growth rate than that with $n = 2$, and the growth rate of the asymmetric disturbance with $n = 2$ is higher than that of the asymmetric disturbance with $n = 3$. Similar observations were reported by Yang (1992) and Avital (1995) in their investigations on the asymmetric instability of Newtonian liquid jets. Goldin et al. (1969) also reached a similar conclusion in their instability investigations of liquid jets. Therefore, it is concluded that for

the given set of parameters, axisymmetric disturbance is more detrimental than asymmetric ones for viscoelastic, Newtonian, and inviscid liquid jets, respectively.

It is seen from inspection of Fig. 2 that for an axisymmetric disturbance ($n = 0$), the growth rate of wave on a viscoelastic liquid jet lies above that corresponding to a Newtonian fluid and below that corresponding to an inviscid fluid. Further inspection shows that for the asymmetric disturbances ($n \neq 0$), this same phenomenon holds true. Hence, this phenomenon is independent of the value of n. Therefore, it is concluded that, in the range of flow parameters associated with the results in Fig. 2, a jet of such a viscoelastic fluid is more unstable than a Newtonian liquid jet, and less unstable than an inviscid jet. Similar results were reported by Goldin et al. (1969) in their studies on the axisymmetric instability of viscoelastic fluid jets. It is inferred that any experimentally observed difference in the instability behavior must, therefore, be due to nonlinear phenomena. Goldin et al. (1969) also reached a similar conclusion in their instability investigations of liquid jets.

It is known that the Ohnesorge number Z and the Reynolds number Re are related to the liquid Weber number We by $We = Z^2Re^2$. When the jet velocity increases the jet inertia force increases, resulting in increase

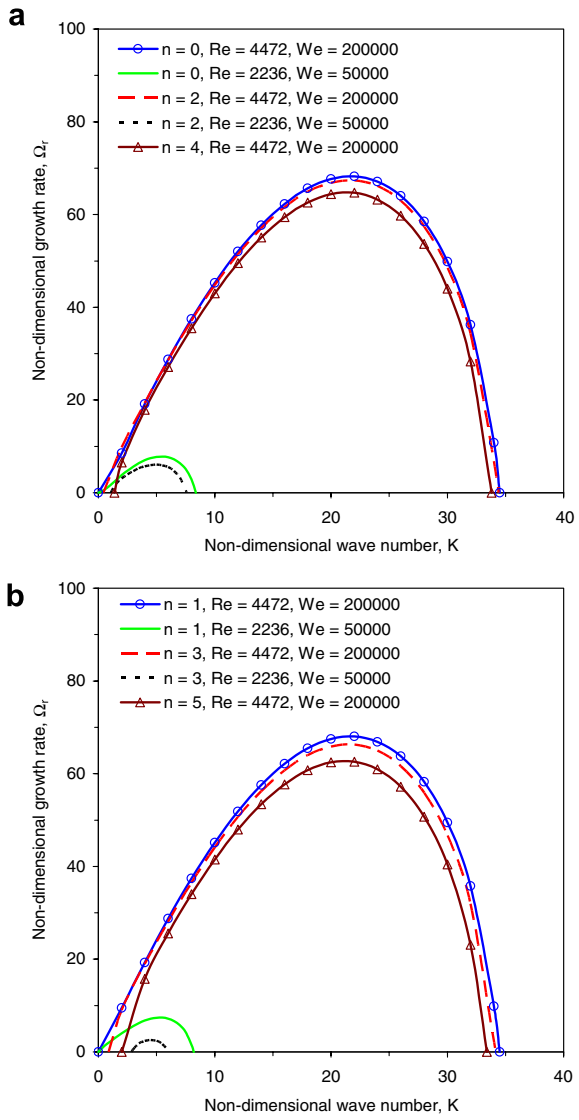

Fig. 3. Effects of the jet velocity on wave growth rate Ω_r of axisymmetric and asymmetric disturbances on viscoelastic liquid jets versus wavenumber K at $Z = 0.1$, $El = 0.1$, $\tilde{\lambda} = 0.1$, $\tilde{\rho} = 0.001$, and $\overline{U}_g = 0$ for (a) $n = 0$, $n = 2$, and $n = 4$, and (b) $n = 1$, $n = 3$, and $n = 5$.

in the corresponding Reynolds number Re and Weber number We. If the jet velocity is doubled from the given conditions in Fig. 2, the corresponding Reynolds number increases from $Re = 2236$ to $Re = 4472$ and the Weber number from $We = 50\,000$ to $We = 200\,000$. The corresponding result, i.e., the effect of the jet velocity (the aerodynamic effect) on wave growth rate of axisymmetric and asymmetric disturbances on viscoelastic liquid jets versus wavenumber K at $Z = 0.1$, $El = 0.1$, $\tilde{\lambda} = 0.1, \tilde{\rho} = 0.001$, and $\overline{U}_g = 0$ is shown in Fig. 3a for $n = 0$, $n = 2$, and $n = 4$, and in Fig. 3b for $n = 1$, $n = 3$, and $n = 5$. From inspection of Fig. 3, it is obvious that as the jet velocity increases, both the growth rate and the instability range increase substantially. Therefore, it is concluded that the aerodynamic effect is the source of the occurrence and growth of the instability on viscoelastic liquid jets, and it strongly influences the instability behavior.

It can be seen from Fig. 3 that the trend continues that the growth rate of the axisymmetric disturbance exceeds that of the asymmetric disturbances and the growth rate of the asymmetric disturbances decreases when the value of n increases. However, the curves of growth rates of all the disturbance modes become very close due to the increase in jet velocity. The maximum growth rate and the corresponding dominant

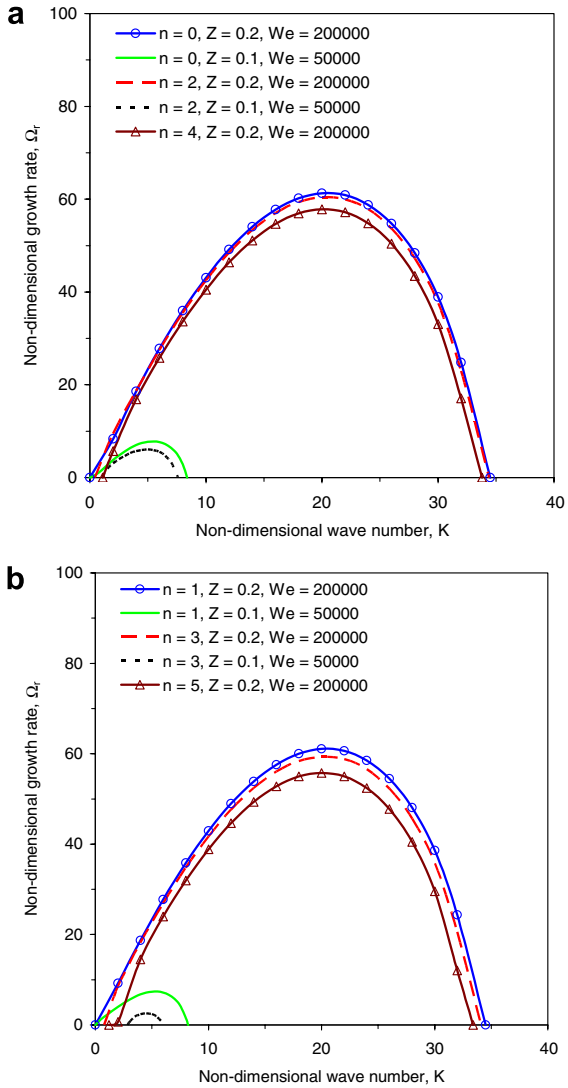

Fig. 4. Effects of the jet surface tension on wave growth rate Ω_r of axisymmetric and asymmetric disturbances on viscoelastic liquid jets versus wavenumber K at $Re = 2{,}236$, $El = 0.1$, $\tilde{\lambda} = 0.1$, $\tilde{\rho} = 0.001$, and $\overline{U}_g = 0$ for (a) $n = 0$, $n = 2$, and $n = 4$, and (b) $n = 1$, $n = 3$, and $n = 5$.

wavenumber for the given conditions in Fig. 3 reduce little with the value of n. This indicates that as the jet velocity increases, the effects of asymmetric disturbance modes on jet breakup enhance drastically, and more asymmetric disturbance modes with large values of n become unstable. In Fig. 3, the disturbance mode effects for $n = 4$ and $n = 5$ are added, and those for $n > 5$ are ignored. Since all these disturbance modes appear on the liquid jet surface during the jet breakup process, the jet breakup process becomes more complicated, which was observed in the experiments by Hoyt and Taylor (1977), and by Lefebvre (1989).

On the other hand, when the jet surface tension decreases the jet surface tension force decreases, resulting in increases in the corresponding Ohnesorge number Z and Weber number We. For example, if the jet surface tension is reduced to one fourth from the given conditions in Fig. 2, the corresponding Ohnesorge number Z increases from $Z = 0.1$ to $Z = 0.2$ and the Weber number increases from $We = 50\,000$ to $We = 200\,000$. Fig. 4 shows the effects of the jet surface tension on wave growth rate of axisymmetric and asymmetric disturbances on viscoelastic liquid jets versus wavenumber K at $Re = 2236$, $El = 0.1$, $\tilde{\lambda} = 0.1$, $\tilde{\rho} = 0.001$, and $\overline{U}_g = 0$ for (a) $n = 0$, $n = 2$, and $n = 4$, and (b) $n = 1$, $n = 3$, and $n = 5$. From inspection of Fig. 4, it can be seen that the effect of jet surface tension on the non-dimensional growth rate is similar to that of the jet velocity. As the jet surface

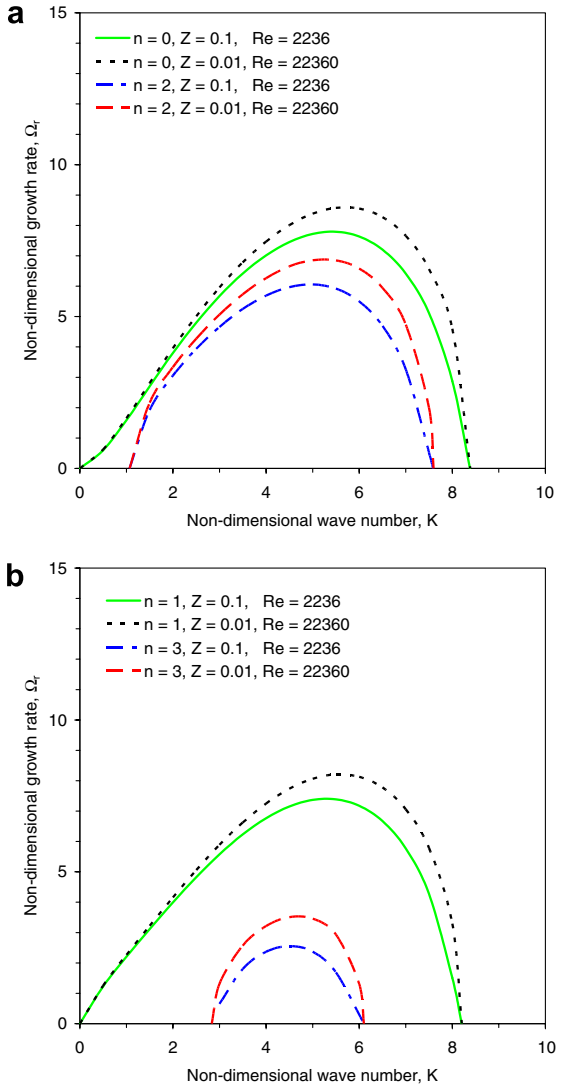

Fig. 5. Effects of the jet viscosity on wave growth rate Ω_r of axisymmetric and asymmetric disturbances on viscoelastic liquid jets versus wavenumber K at $We = 50\,000$, $El = 0.1$, $\tilde{\lambda} = 0.1$, $\tilde{\rho} = 0.001$, and $\overline{U}_g = 0$ for (a) $n = 0$ and $n = 2$, and (b) $n = 1$ and $n = 3$.

tension decreases, both the growth rate and the instability range increase substantially. Therefore, it is concluded that the effect of the jet surface tension resists the occurrence and development of the instability on viscoelastic liquid jets, and it strongly affects the instability behavior.

It also can be seen from Fig. 4 that the growth rate of the axisymmetric disturbance exceeds that of the asymmetric disturbances and the growth rate of the asymmetric disturbances becomes smaller when the value of n increases. Furthermore, the curves of wave growth rate of all the disturbance modes become very close due to the reduced jet surface tension. The maximum growth rate and the corresponding dominant wavenumber for the given conditions in Fig. 4 changes very little with the value of n. This indicates that as the jet surface tension decreases, the effect of asymmetric disturbance modes on jet breakup increases drastically, and more asymmetric disturbance modes with large values of n become unstable. In Fig. 4, the effects of the disturbance modes for $n = 4$ and $n = 5$ are added, and the results of the disturbance modes for $n > 5$ are ignored.

When the jet viscosity is reduced, the corresponding Ohnesorge number Z decreases and the jet Reynolds number Re increases at the same level, with the jet Weber number We unchanged based on their relation. Reducing the jet viscosity to one tenth of the given conditions in Fig. 2 causes the corresponding Ohnesorge number Z to decrease from $Z = 0.1$ to $Z = 0.01$ and the Reynolds number to increase from $Re = 2236$ to $Re = 22\,360$, whereas the Weber number is still kept at $We = 50\,000$. The corresponding results of the effect of the liquid viscosity on wave growth rate Ω_r of axisymmetric and asymmetric disturbances on viscoelastic liquid jets versus wavenumber K at $We = 50\,000$, $El = 0.1$, $\tilde{\lambda} = 0.1$, $\tilde{\rho} = 0.001$, and $\overline{U}_g = 0$ are shown in Fig. 5a for $n = 0$ and $n = 2$, and in Fig. 5b for $n = 1$ and $n = 3$, respectively. From inspection of Fig. 5, it is clear that as the jet viscosity decreases, the growth rates of both axisymmetric and asymmetric disturbances increase. This implies that the jet viscosity can dampen the instability of viscoelastic liquid jets. The maximum growth rate and the dominant wavenumber decrease when the value of n increases. This indicates that asymmetric disturbance effects on the jet instability weaken with n.

From further investigation of Figs. 3–5, it is found that these figures can demonstrate the effects of the jet Weber number We, Reynolds number Re and Ohnesorge number Z on the axisymmetric and asymmetric disturbances of viscoelastic jets. For the same Weber number as shown in Fig. 5, the growth rates of axisymmetric disturbance and each asymmetric disturbance mode change slightly, but the instability ranges do not change with Reynolds number and Ohnesorge number. However, both the growth rates and the instability ranges of axisymmetric disturbance and each asymmetric disturbance mode vary drastically with Weber number for the same Reynolds number shown in Fig. 4 or the same Ohnesorge number shown in Fig. 3.

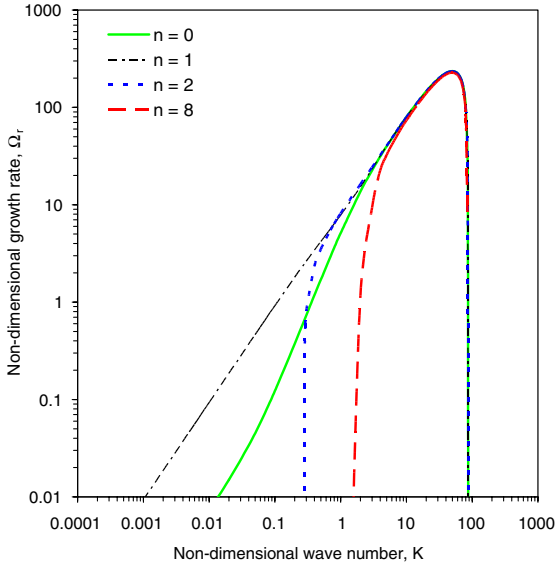

Fig. 6. Effects of the large Weber number on wave growth rate of axisymmetric and asymmetric disturbances on viscoelastic liquid jets versus wavenumber K at $Z = 0.1$, $Re = 7071$, $We = 500\,000$, $El = 0.1$, $\tilde{\lambda} = 0.1$, $\tilde{\rho} = 0.001$, and $\overline{U}_g = 0$.

In addition, it is obvious from Figs. 3 and 4 that the instability ranges of axisymmetric disturbance and each asymmetric disturbance mode are almost identical, and their growth rate amplitudes are of the same order for each corresponding Weber number. It is therefore concluded that the jet Weber number is a key measure that controls the viscoelastic jet instability behavior. It is clear that any parameters that constitute the jet Weber number would influence the jet instability behavior significantly. For example, it is observed from Figs. 3–5 that the effects of jet velocity and surface tension on the wave growth rate of disturbances are much stronger than that of jet viscosity. As a result, in industrial applications such as in fuel sprays in diesel engines, it is extremely difficult to enhance the fuel spray instability through reducing the diesel fuel surface tension. Instead, people increase fuel injection velocity through raising the injection pressure to obtain better fuel atomization and sprays in diesel engines.

For an asymptotic analysis, the Weber number is increased from $We = 50\,000$ to $We = 500\,000$, as shown in Fig. 6. It can be observed from this figure that all the growth rate curves coincide with each other in most of disturbance range, including the asymmetric mode of $n = 8$. However, it should be noted that at small wavenumber, the growth rate of the sinuous disturbances ($n = 1$) is greater than that of the varicose disturbances

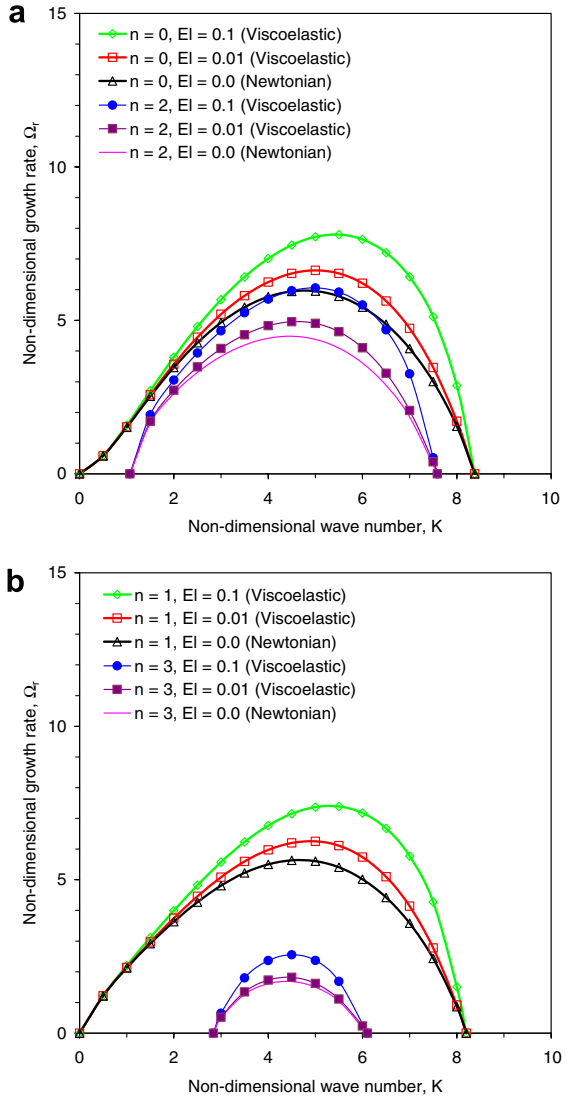

Fig. 7. Effects of the jet elasticity on wave growth rate Ω_r of axisymmetric and asymmetric disturbances on viscoelastic liquid jets versus wavenumber K at $Z = 0.1$, $Re = 2236$, $We = 50000$, $\tilde{\lambda} = 0.1, \tilde{\rho} = 0.001$, and $\overline{U}_g = 0$ for (a) $n = 0$ and $n = 2$, and (b) $n = 1$ and $n = 3$.

($n = 0$). Therefore, it is concluded that for a viscoelastic jet the asymmetric disturbances are more dangerous than that of axisymmetric disturbances at very large Weber numbers.

In order to explore the effects of the liquid elasticity through the elasticity number *El* on the evolution of the instability of viscoelastic liquid jets, the elasticity number is reduced from 0.1 to 0.01, while the other parameters are kept same. The corresponding results are shown in Fig. 7 at $Z = 0.1$, $Re = 2236$, $We = 50000$, $\tilde{\lambda} = 0.1, \tilde{\rho} = 0.001$, and $\overline{U}_g = 0$ (a) for $n = 0$ and $n = 2$, and (b) for $n = 1$ and $n = 3$. It is observed from Fig. 7 that for axisymmetric disturbance and each asymmetric disturbance mode, the wave growth rates decrease as the liquid elasticity is reduced. The wave growth rate curve of disturbances on viscoelastic jets approaches that of the corresponding Newtonian jet. When the elasticity number is reduced to zero, the growth rate curve of viscoelastic jet is transformed into that of Newtonian one, since the fluid has become Newtonian at this condition. Therefore, it is concluded that the liquid elasticity tends to enhance the wave growth rate of disturbances on viscoelastic liquid jets. Thus, it is further confirmed that the linearized

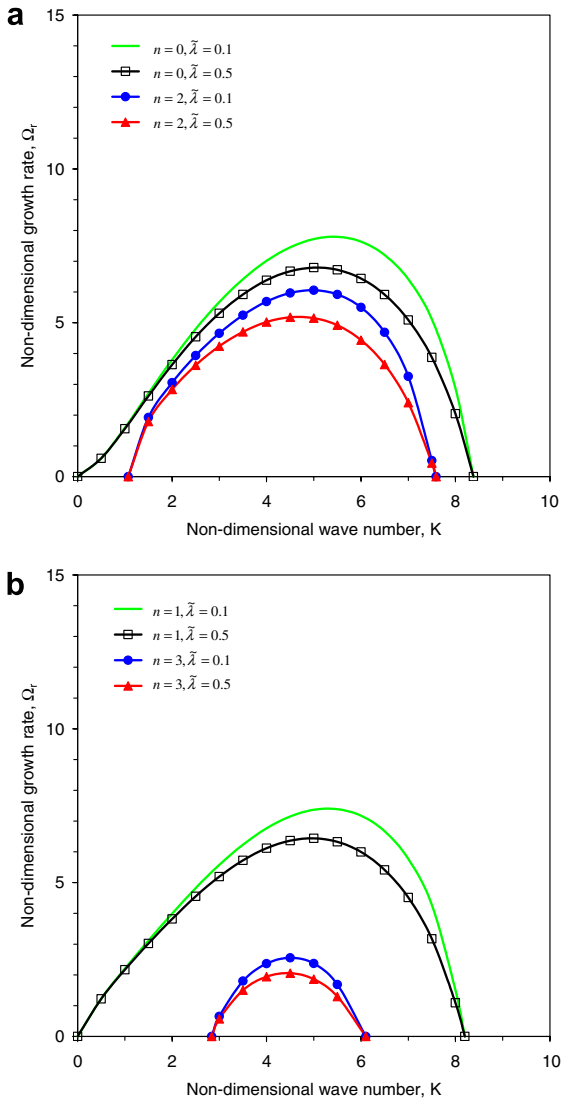

Fig. 8. Effects of the time constant ratio on wave growth rate Ω_r of axisymmetric and asymmetric disturbances on viscoelastic liquid jets versus wavenumber K at $Z = 0.1$, $Re = 2236$, $We = 50000$, $El = 0.1$, $\tilde{\rho} = 0.001$, and $\overline{U}_g = 0$ for (a) $n = 0$ and $n = 2$, and (b) $n = 1$ and $n = 3$.

computations predict viscoelastic liquid jets to be more unstable than Newtonian ones. In addition, the cutoff wavenumber stays same as the elasticity number varies.

The effects of the ratio of deformation retardation to stress relaxation time, $\tilde{\lambda}$, on wave growth rate are presented in Fig. 8 at $Z = 0.1$, $Re = 2236$, $We = 50000$, $El = 0.1$, $\tilde{\rho} = 0.001$, and $\overline{U}_g = 0$ for (a) $n = 0$ and $n = 2$, and (b) $n = 1$ and $n = 3$, respectively. In this figure, the time constant ratio $\bar{\lambda}$ increases from 0.1 to 0.5. It is noticed from Fig. 8 that for axisymmetric disturbance and each asymmetric disturbance mode, the wave growth rate of disturbances decreases as the time constant ratio increases, but the cutoff wavenumber does not change with the time constant ratio.

The effects of the gas to liquid density ratio are examined in Fig. 9a for $n = 0$, $n = 2$, and $n = 4$, and Fig. 9b for $n = 1$, $n = 3$, and $n = 5$ at $Z = 0.1$, $Re = 2236$, $We = 50000$, $El = 0.1$, $\tilde{\lambda} = 0.1$, and $\overline{U}_g = 0$. From inspection of Fig. 9, it is observed that the effects of the gas to liquid density ratio on the growth rates of waves on the viscoelastic jet are significant for both axisymmetric and asymmetric disturbances, similar to the effects of

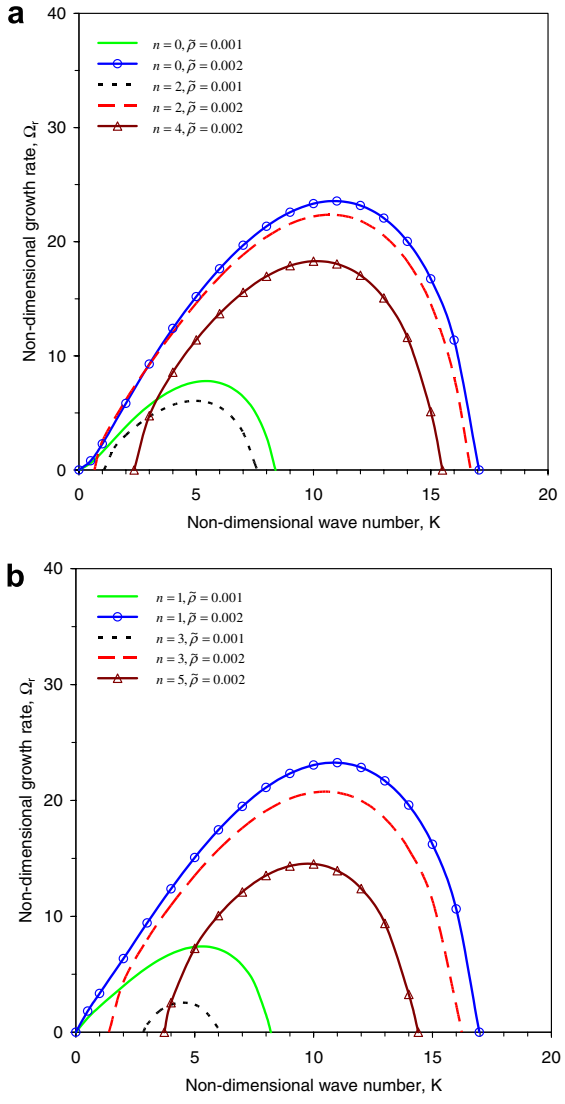

Fig. 9. Effects of the gas to liquid density ratio on wave growth rate Ω_r of axisymmetric and asymmetric disturbances on viscoelastic liquid jets versus wavenumber K at $Z = 0.1$, $Re = 2236$, $We = 50000$, $El = 0.1$, $\tilde{\lambda} = 0.1$, and $\overline{U}_g = 0$ for (a) $n = 0$, $n = 2$, and $n = 4$, and (b) $n = 1$, $n = 3$, and $n = 5$.

the Weber number. When the gas to liquid density ratio is small, the wave growth rate of the axisymmetric disturbance on the viscoelastic jet exceeds that of the asymmetric disturbances and the growth rate of asymmetric disturbances becomes smaller when the value of n increases, indicating the axisymmetric disturbance is more detrimental. When the gas to liquid density ratio increases, both the growth rate and the instability range of disturbances increase drastically, more asymmetric disturbance modes with large values of n become unstable, and the growth rate of each asymmetric disturbance mode approaches that of the axisymmetric disturbance. In Fig. 9, as the gas to liquid density ratio increases from 0.001 to 0.002, we can see that the effects of the disturbance modes for $n = 4$ and $n = 5$ are added, and the effects of the disturbance modes for $n > 5$ are ignored, indicating that at large gas to liquid density ratio, the asymmetric disturbances are gradually becoming more dangerous. Hence, it is concluded that the gas to liquid density ratio is another key measure that controls the viscoelastic jet instability behavior.

In addition, it can be seen from Fig. 9 that the liquid Weber number is unchanged as the gas to liquid density ratio increases, which implies that there is an increase in the gas density ρ_g. Therefore, it is concluded that the high ambient gas density enhances the instability of viscoelastic liquid jets for both axisymmetric and asymmetric disturbances. This agrees well with the practice that people improve the fuel sprays through increasing the gas density in diesel engine cylinders.

4. Conclusions

In this paper, the temporal instability behavior of a viscoelastic liquid jet in the wind-induced regime with axisymmetric and asymmetric disturbances moving in an inviscid gaseous environment is investigated theoretically. As a result of the linear analysis described above, the following conclusions may be drawn.

(1) In the investigated regime, the growth rate of wave on a viscoelastic liquid jet is larger than that of a Newtonian one and smaller than that of an inviscid one for axisymmetric disturbance, and for each asymmetric disturbance mode, this same phenomenon holds true, i.e., this phenomenon is independent of the values of n, indicating that viscoelastic liquid jets are more unstable than their Newtonian counterparts, and less unstable than their inviscid counterparts for both axisymmetric and asymmetric disturbances.

(2) The liquid Weber number is a key measure that controls the viscoelastic jet instability behavior. At small Weber number, the axisymmetric disturbance dominates the instability of viscoelastic jets, i.e., the growth rate of an axisymmetric disturbance exceeds that of the asymmetric disturbances and the growth rate of asymmetric disturbances decreases as the value of n increases. When the Weber number increases, both the growth rate and the instability range of disturbances increase drastically. The asymptotic analysis shows that at large liquid Weber number, more asymmetric disturbance modes with large values of n become unstable, and the growth rate of each asymmetric disturbance mode approaches that of the axisymmetric disturbance in most of disturbance range. In addition, at small wavenumber, the growth rate of the sinuous disturbances ($n = 1$) is greater than that of the varicose disturbances ($n = 0$). Therefore, the asymmetric disturbances are more dangerous than that of the axisymmetric disturbance for viscoelastic jets at large Weber numbers.

(3) Similar to the liquid Weber number, the ratio of gas to liquid density is another key measure that controls the viscoelastic jet instability behavior. When the gas to liquid density ratio is small, the wave growth rate of axisymmetric disturbance is higher than that of asymmetric disturbances, indicating the axisymmetric disturbance is more detrimental. When the gas to liquid density ratio increases, both the growth rate and the instability range of disturbances increase drastically, more asymmetric disturbance modes with large values of n become unstable, and the growth rate of each asymmetric disturbance mode approaches that of the axisymmetric disturbance. Therefore, the effects of the asymmetric disturbances become stronger as the gas to liquid density ratio increases.

(4) The surface tension resists the development of instability on viscoelastic liquid jets with both axisymmetric and asymmetric disturbances, i.e., they smooth out the disturbances on the interface between the liquid and the gas, whereas the aerodynamic effect enhances the instability. These two parameters influence the instability behavior of viscoelastic liquid jets greatly.

(5) For viscoelastic liquid jets the instability behavior is influenced by the interaction of the liquid viscosity and the liquid elasticity, in which the viscosity tends to damp the instability, whereas the elasticity results in an enhancement of instability. However, the viscosity or the elasticity does not change the instability range, indicating that the effect of the viscosity or the elasticity on the instability of viscoelastic liquid jets is weak. In addition, the growth rates of disturbances decrease with the ratio of deformation retardation to stress relaxation time in a relatively weak manner.

Considerably more work is still needed before the complex behavior of viscoelastic fluid jets will be fully understood, and it is hoped that the present work can be a contribution for further investigations of the instability and breakup of viscoelastic liquid jets. At the present time, there is still a lack of nonlinear theoretical results and experimental data in this area. Future work should therefore be directed towards the consideration of nonlinear effects on the destabilization behavior of viscoelastic liquid jets, and corresponding experiments to validate the theoretical results.

References

Avital, E., 1995. Asymmetric instability of a viscid capillary jet. Phys. Fluids 7, 1162–1164.

Batchelor, G.K., Gill, A.E., 1962. Analysis of the stability of axisymmetric jets. J. Fluid Mech. 14, 529–551.

Bird, R.B., Armstrong, R.C., Hassager, O., 1977. Dynamics of Polymeric Liquids. In: Fluid Mechanics, vol. 1. John Wiley & Sons, New York.

Bogy, D.B., 1979. Drop formation in a circular liquid jet. Ann. Rev. Fluid Mech. 11, 207–228.

Brenn, G., Liu, Z., Durst, F., 2000. Linear analysis of the temporal instability of axisymmetrical non-Newtonian liquid jets. Int. J. Multiphase Flow 26, 1621–1644.

Chigier, N.A., Reitz, R.D., 1996. Regimes of jet breakup and breakup mechanisms. Progress Astronaut. Aeronaut. 1, 109–136.

Darby, R., 1976. Viscoelastic Fluids. Marcel Dekker, New York.

Giffen, E., Muraszew, A., 1953. The Atomization of Liquid Fuels. John Wiley & Sons, New York.

Goedde, E.F., Yuen, M.C., 1970. Experiments on liquid jet instability. J. Fluid Mech. 40, 495–512.

Goldin, M., Yerushalmi, J., Pfeffer, R., Shinnar, R., 1969. Breakup of a laminar capillary jet of a viscoelastic fluid. J. Fluid Mech. 38, 689–711.

Gordillo, J.M., Perez-Saborid, M., 2005. Aerodynamic effects in the break-up of liquid jets: on the first wind-induced break-up regime. J. Fluid Mech. 541, 1–20.

Gordon, M., Yerushalmi, J., Shinnar, R., 1973. Instability of jets of non-Newtonian fluids. Trans. Soc. Rheol. 17, 303–324.

Goren, S., Gottlieb, M., 1982. Surface-tension-driven breakup of viscoelastic liquid threads. J. Fluid Mech. 120, 245–266.

Grant, R.P., Middleman, S., 1966. Newtonian jet stability. AIChE J. 12, 669–678.

Hoyt, J.W., Taylor, J.J., 1977. Waves on water jets. J. Fluid Mech. 83, 119–127.

Kroesser, F.W., Middleman, S., 1969. Viscoelastic jet stability. AIChE J. 15, 383–386.

Lefebvre, A.H., 1989. Atomization and Sprays. Hemisphere, New York.

Li, X., 1995. Mechanism of atomization of a liquid jet. Atomization Sprays 5, 89–105.

Lian, Z.W., Reitz, R.D., 1993. The effects of vaporization and gas compressibility on liquid jet atomization. Atomization Sprays 3, 249–264.

Lin, S.P., Ibrahim, E.A., 1990. Instability of a viscous liquid jet surrounded by a viscous gas in a vertical pipe. J. Fluid Mech. 218, 641–658.

Lin, S.P., Kang, D.J., 1987. Atomization of a liquid jet. Phys. Fluids 30, 2000–2006.

Lin, S.P., Lian, Z.W., 1990. Mechanism of the breakup of liquid jets. AIAA J. 28, 120–126.

Liu, Z., Brenn, G., Durst, F., 1998. Linear analysis of the instability of two-dimensional non-Newtonian liquid sheets. J. Non-Newtonian Fluid Mech. 78, 133–166.

Liu, Z., Liu, Z., 2006. Linear analysis of three-dimensional instability of non-Newtonian liquid jets. J. Fluid Mech. 559, 451–459.

McCarthy, M.J., Molloy, N.A., 1974. Review of stability of liquid jets and the influence of nozzle design. Chem. Eng. J. 7, 1–20.

Meister, B.J., Scheele, G.F., 1969. Prediction of jet length in immiscible liquid systems. AIChE J. 15, 689–699.

Middleman, S., 1965. Stability of a viscoelastic jet. Chem. Eng. Sci. 20, 1037–1040.

Muller, D.E., 1956. A method for solving algebraic equations using an automatic computer. Math. Tables Aids Comput. 10, 208–215.

Park, H.M., Lee, H.S., 1995. Nonlinear hydrodynamic stability of viscoelastic fluids heated from below. J. Non-Newtonian Fluid Mech. 60, 1–26.

Phinney, R.E., 1973. Stability of a laminar viscous jet. The influence of an ambient gas. Phys. Fluids 16, 193–196.

Rayleigh, L., 1878. On the instability of jets. Proc. Lond. Math. Soc. 10, 4–13.

Rayleigh, L., 1879. On the capillary phenomena of jets. Proc. Roy. Soc. London A 29, 71–97.

Rayleigh, L., 1892. On the instability of a cylinder of viscous liquid under capillary force. Phil. Mag. 34, 145–154.

Reitz, R.D., Bracco, F.V., 1982. Mechanism of atomization of a liquid jet. Phys. Fluids 25, 1730–1742.

Schowalter, W.R., 1978. Mechanics of Non-Newtonian Fluids. Pergamon Press, Oxford.

Sterling, A.M., Sleicher, C.A., 1975. The instability of capillary jets. J. Fluid Mech. 68, 477–495.

Weber, C., 1931. Zum Zerfall eines Flüssigkeitsstrahles. Z. Angew Math. Mech. 11, 136–154.
Yang, H.Q., 1992. Asymmetric instability of a liquid jet. Phys. Fluids A 4, 681–689.
Yarin, A.L., 1993. Free Liquid Jets and Films: Hydrodynamics and Rheology. John Wiley & Sons, New York.
Yuen, M.C., 1968. Nonlinear capillary instability of a liquid jet. J. Fluid Mech. 33, 151–163.
Zhou, Z.W., Lin, S.P., 1992. Effects of compressibility on the atomization of liquid jets. AIAA J. Propulsion Power 8, 736–740.